

Dynamic Properties of Cyclohexane Guest Molecules Constrained within the Zeolite H-ZSM-5 Host Structure: A Wide-Line Solid State ^2H NMR Investigation

Abil E. Aliev[†] and Kenneth D. M. Harris^{*‡}

Department of Chemistry, University College London, 20 Gordon Street, London WC1H 0AJ, U.K., and School of Chemistry, University of Birmingham, Edgbaston, Birmingham B15 2TT, U.K.

Received: January 8, 1997; In Final Form: March 10, 1997[⊗]

Dynamic properties of perdeuterated cyclohexane (C_6D_{12}) molecules included within the zeolite H-ZSM-5 host structure have been studied by variable-temperature wide-line solid-state ^2H NMR spectroscopy. Three types of rapid motion have been identified for the C_6D_{12} molecules in the temperature range 93–233 K as follows: motion A, rapid reorientation about the C_3 symmetry axis of the C_6D_{12} molecule; motion B, rapid restricted wobbling of the C_3 symmetry axis, described as precession of the C_3 symmetry axis on the surface of a cone (the half angle of which increases with increasing temperature); motion C, a rapid four-site jump motion, the geometry of which is dictated by the orientations of the tunnel axes at the intersection between the zigzag and straight tunnels of the H-ZSM-5 host structure. The temperature dependence of the quadrupole echo ^2H NMR line shape in the temperature range 263–368 K is interpreted in terms of cyclohexane ring inversion occurring in the intermediate motion regime, in addition to motions A–C, which are in the rapid motion regime. From the ^2H NMR line shape analysis, the activation energy for the cyclohexane ring inversion process is estimated to be ca. 48 kJ mol⁻¹. The dynamic properties are compared with those of cyclohexane in other solid host structures, and the constraints imposed by the H-ZSM-5 host structure on the dynamic properties of the cyclohexane guest molecules are assessed.

1. Introduction

Much of the impetus underlying current research on solid inclusion compounds is driven by the desire to understand the ways in which properties may be conferred upon organic guest molecules by virtue of embedding them within a solid host structure. Properties of the guest molecules that have been investigated widely in this regard include the conformational properties (importantly, guest molecules included within a solid host structure are often constrained to exhibit uncharacteristic conformational behavior) and the dynamic properties, as discussed in more detail below. A wide range of host structures are available for such studies, and the fact that they differ substantially in their structural and chemical properties provides a basis for determining which factors play a major role in controlling the properties of the guest molecules. Examples of solid host structures are aluminosilicates (including zeolites and clays), aluminophosphates, layered chalcogenides, and layered metal phosphonates, as well as crystalline organic host solids such as urea, thiourea, tri-*o*-thymotide, perhydrotriphenylene, and deoxycholic acid. The topologies of the “inclusion cavities” within these host solids are varied and encompass linear tunnel structures, isolated cages, networks of intersecting tunnels and/or cages, and two-dimensional regions within layered hosts.

Guest molecules within solid host structures usually undergo a variety of dynamic processes that reflect, to a greater or lesser extent, the structural attributes of the host structure and the physical constraints imposed by the host structure. Different dynamic processes occur on different characteristic time scales, and a range of experimental and computational techniques are therefore required to study the dynamic properties of the guest molecules in different systems. One of the most extensively used techniques in this regard has been wide-line solid-state

^2H NMR spectroscopy,^{1–4} based on the fact that ^2H NMR line shape analysis is a particularly sensitive probe of molecular motions with characteristic time scales in the range 10^{-3} – 10^{-7} s (the so-called “intermediate motion regime”). For motions with time scales in this range, ^2H NMR line shape analysis can generally allow the mechanism and rate of motion to be established, with the temperature dependence of the rate of motion leading to information on activation parameters. If the characteristic time scale of the motion is shorter than 10^{-7} s (the so-called “rapid motion regime”), details of the exact rate of motion cannot be established, although ^2H NMR line shape analysis can, in general, still provide detailed information on the geometry and mechanism of the motion. Since the characteristic time scales of reorientational motions of guest molecules in solid inclusion compounds are often within the range probed by ^2H NMR line shape analysis, this technique has been applied widely to study the dynamic properties of such inclusion compounds.

The dynamic properties of cyclohexane guest molecules have been investigated in a range of solid inclusion compounds, such as the thiourea host structure,⁵ the Cd(CN)₂ host structure,² and the Cd(mtn)Ni(CN)₄ [mtn = CH₃NH(CH₂)₃NH₂] host structure.⁶ It is interesting to note that the ^2H NMR line shape reported at 103 K for C_6D_{12} in the Cd(CN)₂ host structure is almost identical with the line shape observed at 93 K in the present paper for C_6D_{12} in the H-ZSM-5 host structure. However, full details of the dynamic model responsible for the observed line shape in the case of C_6D_{12} /Cd(CN)₂ were not reported in ref 2. To our knowledge, only limited information is available regarding the dynamic properties of cyclohexane in zeolitic host structures and has so far been confined to experimental ^2H NMR studies⁷ of the dynamics of C_6D_{12} guest molecules in zeolite L, with only a qualitative analysis of the temperature dependence of the observed ^2H NMR line shape. From the ^2H NMR spectra reported for C_6D_{12} in zeolite L, it is clear that the ^2H NMR line shape and its temperature dependence (and hence, the dynamic

* To whom all correspondence should be addressed.

[†] University College London.

[‡] University of Birmingham.

[⊗] Abstract published in *Advance ACS Abstracts*, May 15, 1997.

properties of the C₆D₁₂ guest molecules) are different from those reported here for the same guest molecules in the H-ZSM-5 host structure.

In this paper we report the dynamic properties of perdeuterated cyclohexane guest molecules included within the zeolitic host H-ZSM-5. This work provides a basis for comparing the dynamic properties of cyclohexane in H-ZSM-5 with the dynamic properties of the same guest molecule in other solid host structures and allows an assessment of the constraints imposed by the H-ZSM-5 host structure on the dynamic properties of guest molecules within it. The framework structure of ZSM-5^{8,9} contains a set of zigzag tunnels intersecting a set of straight tunnels, each with 10-membered ring openings. The diameter of the straight tunnel ranges between ca. 5.4 and 5.6 Å, and the diameter of the zigzag tunnel ranges between ca. 5.1 and 5.5 Å. The angle between the tunnel axes of adjacent segments of the zigzag tunnel is 112.7°.

Although the H⁺ form of ZSM-5 has been used in this work, it is considered unlikely that the dynamic properties of the C₆D₁₂ guest molecules will differ significantly depending on the nature of the extraframework cation or depending on the number of acidic sites on the zeolite framework. Indeed, as discussed previously,⁷ strong interactions between an aluminosilicate host structure (zeolite L) and the guest molecules may be expected for guest molecules (e.g., benzene) that possess π -electron density and interact strongly with the extraframework cations. Such cation effects were also studied in detail in a subsequent report¹⁰ for different guest molecules (benzene, hexane, and cyclohexane) and samples of zeolite L containing different extraframework cations (Li⁺, K⁺, Cs⁺). For benzene and hexane, it was found that the size of the cation influences significantly the steric environment of the guest molecules, whereas in the case of cyclohexane, the nature of the cation has a substantially smaller effect on the dynamic properties of the guest molecules. In summary, cyclohexane guest molecules are unlikely to be affected significantly (in contrast, for example, to the case for benzene and *p*-xylene¹¹) by the chemical properties of the H-ZSM-5 host structure, and as such, cyclohexane serves as a valuable probe of the physical constraints imposed by the zeolite framework structure.

Clearly, in the case of C₆D₁₂ guest molecules, with two different deuteron positions (axial and equatorial) and a possible combination of several different types of molecular motion, it is not satisfactory to attempt to rationalize observed ²H NMR line shapes solely through qualitative analyses based on simple analytical expressions (of the type considered in refs 2 and 7). Instead, we believe that a comprehensive understanding of the dynamic properties (at least in the case of complex, multicomponent motions) can be obtained only through detailed numerical calculations to simulate the observed ²H NMR line shapes and their temperature dependence, allowing the relative validity of different plausible dynamic models to be assessed objectively and critically. Thus, this approach has been adopted in our analysis of the ²H NMR spectra for the C₆D₁₂/H-ZSM5 system reported here. We note that such an approach would enhance considerably the present level of understanding of the dynamic properties of C₆D₁₂ guest molecules in other host materials, such as Cd(CN)₂² and zeolite L^{7,10} discussed above.

2. Experimental Section

The sample of H-ZSM-5 (Laporte Inorganics, RD1136/88) used in this work was calcined in a muffle furnace at 500 °C for over 24 h before use. Perdeuterated cyclohexane (denoted C₆D₁₂) was obtained commercially and was used without further purification. The C₆D₁₂/H-ZSM-5 inclusion compound was

prepared by contacting ca. 5 cm³ of liquid C₆D₁₂ with ca. 1 g of powdered H-ZSM-5 in a round-bottomed flask under vacuum for ca. 3 days. After this time, the excess liquid was removed under vacuum and the solid was allowed to dry. The flask was sealed and removed to a drybox, within which the solid was transferred to the sample holders used for the solid-state NMR experiments. It has been demonstrated previously¹² by appropriate control experiments that this method of preparation of the C₆D₁₂/H-ZSM-5 inclusion compound leads to adsorption of C₆D₁₂ on the internal surfaces (rather than the external surfaces) of the H-ZSM-5 host material. From elemental analysis (carbon percentage), the loading of C₆D₁₂ guest molecules within the H-ZSM-5 host structure in the sample of C₆D₁₂/H-ZSM-5 used in this work is estimated to be 3.0 guest molecules per unit cell (which corresponds, on average, to 0.75 guest molecules per intersection site between the zigzag and straight tunnels).

²H NMR spectra of C₆D₁₂/H-ZSM-5 were recorded at 46.1 MHz on a Bruker MSL300 spectrometer, using standard Bruker 5 mm high-power probes. The stability and accuracy of the temperature controller (Bruker B-VT1000) were ca. ± 2 K. ²H NMR spectra were recorded using the conventional quadrupole echo [(90°) _{ϕ} – τ –(90°) _{$\phi \pm \pi/2$} – τ –acquire–recycle] pulse sequence¹³ with 90° pulse duration in the range 2.0–3.3 μ s and echo delays $\tau = 13 \mu$ s and $\tau = 200 \mu$ s. Note that no spectral distortions occur within this range of τ , and such distortions are observed only for $\tau < 10 \mu$ s for the probe used. The recycle delay was taken as ca. 5T₁ and ranged from 1 to 20 s depending upon the temperature. Phase cycling was employed to eliminate quadrature phase errors.

3. Simulation and Interpretation of ²H NMR Spectra

Simulations of ²H NMR spectra for motions occurring in the rapid motion regime were carried out using the program FASTPOWDER.¹⁴ Simulations of ²H NMR spectra for C₆D₁₂ ring inversion in the intermediate motion regime were carried out using a version of the ²H NMR simulation program MXQET¹⁵ modified to allow calculation of ²H NMR spectra in the case of the exchange of deuterons between sites with different quadrupole coupling constants and different asymmetry parameters. The quality of the agreement between the simulated and experimental spectra was assessed objectively on the basis of the following function:

$$R = 100 \left(\frac{\sum_{i=1}^M (I_i^{\text{exp}} - I_i^{\text{calc}})^2}{\sum_{i=1}^M (I_i^{\text{exp}})^2} \right)^{1/2}$$

where I_i^{exp} is the intensity of the *i*th digitized data point in the experimental spectrum (*i* = 1, 2, ..., *M*) and I_i^{calc} is the intensity of the *i*th digitized data point in the calculated spectrum. Typical values of *R* for the best fits between the simulated and experimental spectra were between 3% and 7%. We emphasize that this approach provides an objective assessment of the level of agreement between experimental and simulated ²H NMR spectra and removes much of the subjectivity that is characteristic of the traditional approach of comparing experimental and simulated ²H NMR spectra “by eye”.

In modeling dynamic processes, each ²H site involved in the motion can be defined by the Euler angles { α , β , γ }, which specify the orientation (relative to a space-fixed reference frame) of the principal axis system of the electric field gradient (EFG) tensor at the ²H nucleus (we use \mathbf{V}^{PAS} to denote the EFG tensor

in its principal axis system at the ^2H nucleus). Note the following: (a) the components of \mathbf{V}^{PAS} are taken such that $|V_{zz}| \geq |V_{yy}| \geq |V_{xx}|$; (b) the static quadrupole coupling constant χ is defined as e^2Qq_{zz}/h (where Q is the electric quadrupole moment of the nucleus and $eq_{zz} = V_{zz} = \partial^2V/\partial z^2$ is the largest principal component of the EFG tensor at the nucleus); (c) the static asymmetry parameter η is defined as $\eta = (|V_{yy}| - |V_{xx}|)/|V_{zz}|$ and is in the range $0 \leq \eta \leq 1$ [note that since the \mathbf{V}^{PAS} tensor is traceless, $V_{zz} = -(V_{xx} + V_{yy})$]; (d) the z -axis of \mathbf{V}^{PAS} is assumed to lie along the direction of the C–D bond.

The values of the static ^2H quadrupole coupling constant and the static ^2H asymmetry parameter for solid cyclohexane obtained from ^2H NMR studies of a polycrystalline sample at 77 K have been reported previously¹⁶ to be $\chi = 174$ kHz and $\eta = 0.0$, and these value of χ and η are assumed in the present work. Note that other experimental assessments of these parameters are in close agreement (for example,¹⁷ $\chi = 173.7$ kHz and $\eta \leq 0.01$).

Many of the ^2H NMR spectra reported here represent motions that are rapid (i.e., occurring at frequencies greater than ca. 10^7 Hz) relative to the ^2H NMR time scale. In general, ^2H NMR line shapes in the rapid motion regime can be simulated as though they are “static” spectra by using a motionally averaged (“effective”) quadrupole coupling constant (denoted χ^*) and a motionally averaged (“effective”) asymmetry parameter (denoted η^*) and assuming no motion of the effective deuteron. In general, χ^* and η^* differ from the static quadrupole coupling constant (χ) and the static asymmetry parameter (η). Furthermore, in considering such spectra to be represented by an effective static deuteron (with quadrupole interaction parameters χ^* and η^*), the orientation of the principal axis system of the EFG tensor for this effective deuteron generally differs from the orientation of the principal axis system of the EFG tensor for the true static deuteron (with quadrupole interaction parameters χ and η). In much of the subsequent discussion, it is convenient to discuss ^2H NMR spectra for motions occurring in the rapid motion regime in terms of the effective quadrupole interaction parameters χ^* and η^* .

4. Results and Discussion

Figures 1–4 show ^2H NMR spectra of $\text{C}_6\text{D}_{12}/\text{H-ZSM-5}$ recorded at various temperatures between 93 and 368 K. At 93 K, the ^2H NMR line shape is not a Pake powder pattern characteristic of deuterons that are static (or undergoing motion that is slow with respect to the ^2H NMR time scale). Thus, it is clear that motion is occurring that is intermediate or rapid with respect to the ^2H NMR time scale. At 93 K, the ^2H NMR line shape is independent of the echo delay τ , suggesting that the dynamic process is not in the intermediate motion regime and must therefore be in the rapid motion regime. The observed line shape at 93 K can be considered as a superposition of two contributions: a “central part” with line width of ca. 28 kHz and a “wide part” with line width of ca. 85 kHz, with the ratio of these line widths close to 1:3. This situation is characteristic of a C_6D_{12} molecule undergoing rapid reorientation about its C_3 symmetry axis (motion A; see below), as observed for the $\text{C}_6\text{D}_{12}/\text{thiourea}$ ⁵ and $\text{C}_6\text{D}_{12}/\text{Cd}(\text{CN})_2$ ² inclusion compounds. On the basis of this dynamic model, the central part with line width of ca. 28 kHz is assigned to equatorial deuterons and the wide part with line width of ca. 85 kHz is assigned to axial deuterons. For this dynamic model, the ratio $\chi^*(\text{eq})/\chi^*(\text{ax})$ is independent of temperature and is consistent with the observation, from our experimental results, that although the line widths of the central part and the wide part decrease gradually on increasing the temperature from 93 to 233 K, the ratio of these line widths

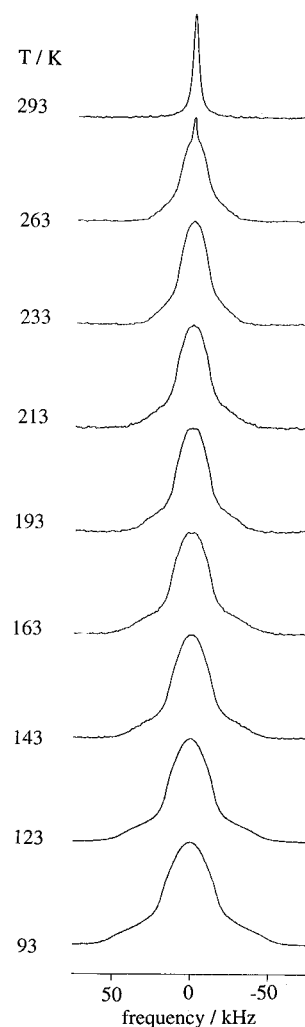


Figure 1. Experimental ^2H NMR spectra for $\text{C}_6\text{D}_{12}/\text{H-ZSM-5}$ recorded with echo delay $\tau = 13 \mu\text{s}$ between 93 and 293 K.

remains constant at ca. 1:3. Thus, the ^2H NMR spectra are consistent with the expectation that ring inversion of the C_6D_{12} guest molecules (which would interconvert axial and equatorial deuteron environments) is slow with respect to the ^2H NMR time scale in the temperature range 93–233 K.

Rapid reorientation of the C_6D_{12} molecule about its C_3 symmetry axis alone cannot account for the ^2H NMR spectrum of $\text{C}_6\text{D}_{12}/\text{H-ZSM-5}$ in the range 93–233 K, and it is necessary to invoke additional motions. After considering a wide range of plausible dynamic models, the following combination of motions was found to give a good account of the ^2H NMR spectra in the temperature range 93–233 K. We recall that, in describing these dynamic processes as rapid, the characteristic time scale of these motions is less than 10^{-7} s.

Motion A is a rapid reorientation of the C_6D_{12} molecule about its C_3 symmetry axis, which we represent as a nearest-neighbor $2\pi/3$ jump motion. From spectral simulations for motion A and by use of the static quadrupole interaction parameters $\chi = 174$ kHz and $\eta = 0.0$, the motionally averaged quadrupole interaction parameters are $\chi^*(\text{ax}) = 173.7$ kHz, $\eta^*(\text{ax}) = 0$ for the axial deuterons ($\theta = 2.1^\circ$) and $\chi^*(\text{eq}) = 56.1$ kHz, $\eta^*(\text{eq}) = 0$ for the equatorial deuterons ($\theta = 71.5^\circ$). In each case, θ denotes the angle between the C_3 symmetry axis (rotation axis) of the C_6D_{12} molecule and the z -axis of the (static) \mathbf{V}^{PAS} tensor (the direction of the C–D bond), with the molecular geometry taken from MM2 calculations. For both axial and equatorial deuterons, the z -axis of the \mathbf{V}^{PAS} tensor for the “effective”

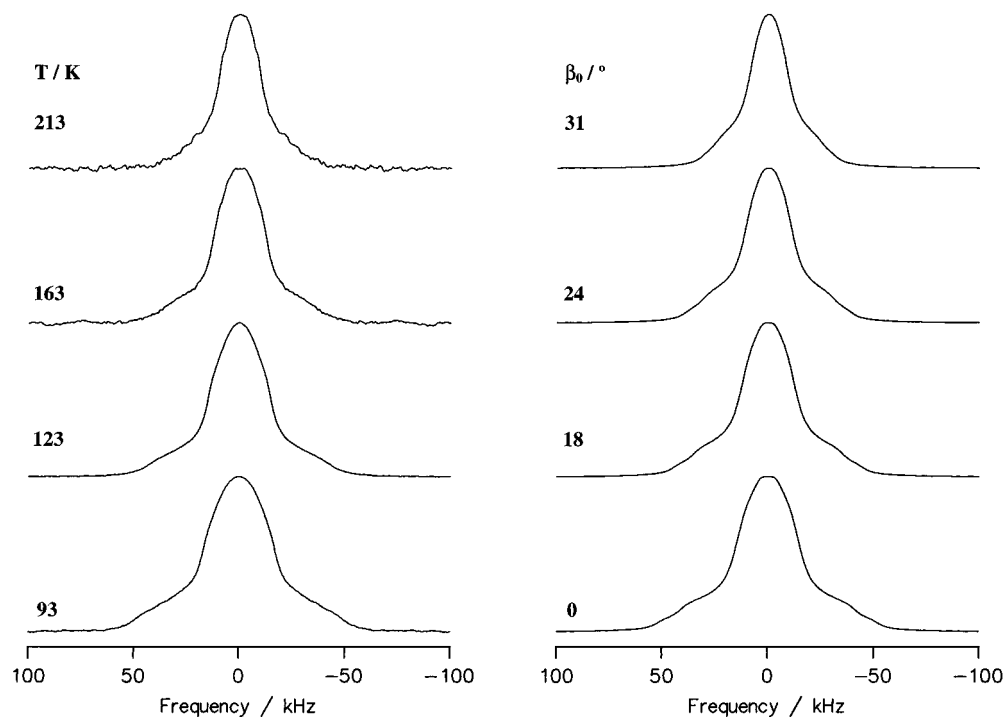


Figure 2. Experimental (left side) and simulated (right side) ^2H NMR spectra for $\text{C}_6\text{D}_{12}/\text{H-ZSM-5}$ recorded with echo delay $\tau = 13 \mu\text{s}$. The simulated spectra were calculated using the combination of motions A–C discussed in the text. The temperature at which each experimental spectrum was recorded and the cone half angle β_0 for motion B used in calculating each spectrum are shown. All simulated spectra shown are for $p_1 = 0.3$.

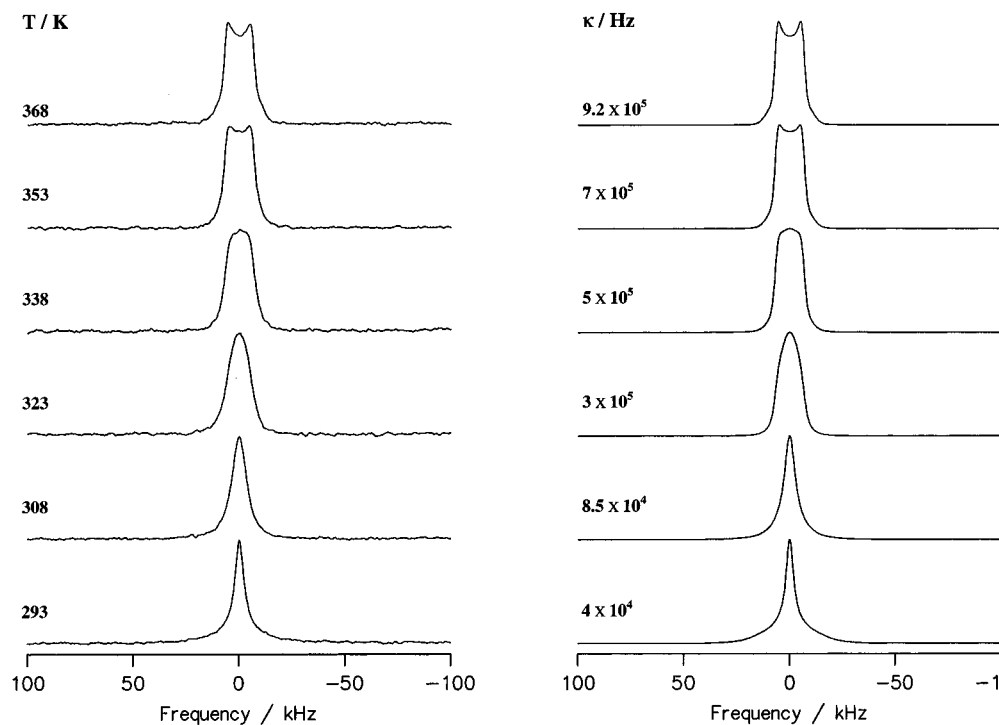


Figure 3. Experimental (left side) and simulated (right side) ^2H NMR spectra for $\text{C}_6\text{D}_{12}/\text{H-ZSM-5}$ recorded with echo delay $\tau = 13 \mu\text{s}$. The simulated spectra were calculated assuming the cyclohexane ring inversion process (in addition to motions A–C) discussed in the text. The temperature at which each spectrum was recorded and the rate (κ) of the cyclohexane ring inversion process used in calculating each spectrum are shown.

deuteron resulting from motion A in the rapid motion regime lies along the rotation axis (i.e., the molecular C_3 symmetry axis).

Motion B is a rapid reorientation of the C_3 symmetry axis of the C_6D_{12} molecule on the surface of a cone of half-angle β_0 (this type of motion is often described as “wobbling”). In the spectral simulations reported here, this dynamic process has been represented as a nearest-neighbor $2\pi/36$ jump motion between 36 orientations of the C_3 symmetry axis equally spaced on the

surface of the cone. For this model,¹⁸ the effective quadrupole coupling constant χ^* is proportional to $(3 \cos^2 \beta_0 - 1)/2$. When motion B is combined with motion A, the value of χ^* is decreased below that for only motion A (with the value of χ^* decreasing as β_0 is increased). The z -axes of the effective \mathbf{V}^{PAS} tensors for both the axial and equatorial deuterons lie along the axis of the cone, although clearly the magnitude of χ^* is different for the axial and equatorial deuterons.

Motion C is rapid four-site jumps of the z -axis of the effective

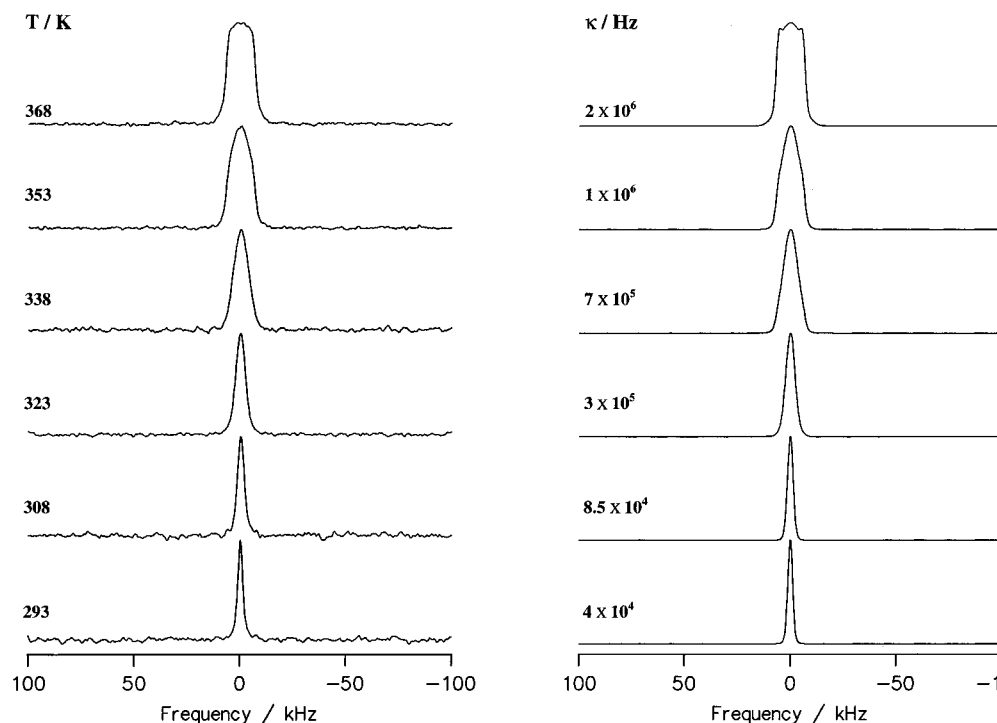
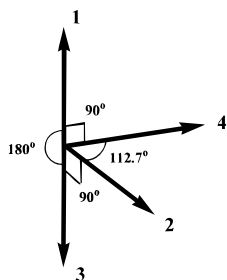


Figure 4. Experimental (left side) and simulated (right side) ^2H NMR spectra for $\text{C}_6\text{D}_{12}/\text{H-ZSM-5}$ recorded with echo delay $\tau = 200 \mu\text{s}$. The simulated spectra were calculated assuming the cyclohexane ring inversion process (in addition to motions A–C) discussed in the text. The temperature at which each spectrum was recorded and the rate (κ) of the cyclohexane ring inversion process used in calculating each spectrum are shown.

\mathbf{V}^{PAS} tensor for the combined motions A and B. The four orientations of the z -axis of the effective \mathbf{V}^{PAS} tensor are shown below:



The angles $\phi(m,n)$ between each pair of orientations m and n are the following: $\phi(1,2) = 90^\circ$; $\phi(1,3) = 180^\circ$; $\phi(1,4) = 90^\circ$; $\phi(2,3) = 90^\circ$; $\phi(2,4) = 112.7^\circ$; $\phi(3,4) = 90^\circ$. For this set of orientations, simulated ^2H NMR spectra in the rapid motion regime are the same for nearest-neighbor exchange ($1 \leftrightarrow 2 \leftrightarrow 3 \leftrightarrow 4 \leftrightarrow 1$) and for all-sites exchange processes. The geometrical relationship between these orientations is closely associated with the geometrical relationship between the orientations of the tunnel axes at the intersection of the zigzag and straight tunnels in the H-ZSM-5 host structure. If we consider, at least initially, that the C_6D_{12} molecules reside preferentially at the intersections of the zigzag and straight tunnels, the orientations involved in motion C can be interpreted readily in terms of the z -axis of the effective \mathbf{V}^{PAS} tensor pointing toward the “entrances” to the tunnels: orientations 1 and 3 are directed toward the entrances to the straight tunnel, whereas orientations 2 and 4 are directed toward the entrances to the zigzag tunnel. Owing to the differences in the diameters and the shapes of the two types of tunnel, we should in general expect the populations of orientations 1 and 3 to be different from the populations of orientations 2 and 4. Thus, $p_1 = p_3$ and $p_2 = p_4 = 1/2 - p_1$ (with $\sum_i p_i = 1$). The proposal that the C_6D_{12} guest molecules reside preferentially at the intersections of the zigzag and straight

tunnels is consistent with the results of preliminary computational investigations of $\text{C}_6\text{D}_{12}/\text{H-ZSM-5}$, which will be the subject of a detailed future paper.¹⁹ As discussed in more detail in section 5, the proposed dynamic model for motion C does not in fact require that the C_6D_{12} guest molecules are located only at the intersection sites but rather that if the guest molecules translate into the tunnels, reorientation of the z -axis of the effective \mathbf{V}^{PAS} tensor occurs only when the guest molecules encounter the intersection sites.

From comparison of the ^2H NMR line shapes simulated for the combination of motions A–C in the rapid motion regime with the experimental ^2H NMR spectrum at 93 K, the values of β_0 and p_1 are estimated to be 0° and 0.3, respectively (Figure 2). Thus, motion B has no significant effect on the line shape at 93 K, and since $p_1 > p_2$ for motion C, the C_3 axis of the C_6D_{12} guest molecule has a preferential orientation in the direction of the straight tunnel rather than the zigzag tunnel. The experimental spectra recorded at 123, 163, and 213 K have been considered in detail in order to estimate the amplitude of motion B at higher temperatures, with the values of β_0 and p_1 varied in the spectral simulations. The best fits (Figure 2) between the experimental and simulated spectra are found for β_0 values of 18° , 24° , and 31° at 123, 163, and 213 K, respectively, and with $p_1 = 0.3$ at all temperatures. As expected, the value of β_0 , and hence, the effective amplitude of the wobbling motion, increases with increasing temperature.

Qualitatively, new line shape changes are observed in the ^2H NMR spectra recorded at temperatures between 263 and 368 K (Figures 1 and 3). Furthermore, the ^2H NMR spectra recorded between 293 and 368 K demonstrate a clear dependence on the echo delay τ (see Figures 3 and 4). At 293 K, for example, the observed line shape is nearly Lorentzian with line width $\Delta\nu_{1/2} = 3.6$ kHz for echo delay $\tau = 13 \mu\text{s}$ and is nearly Gaussian with $\Delta\nu_{1/2} = 1.4$ kHz for echo delay $\tau = 200 \mu\text{s}$ (Figures 3 and 4). Although the observed line shape at 293 K resembles the characteristic line shape for rapid isotropic motion, this possibility can be rejected by the fact that, for temperatures above

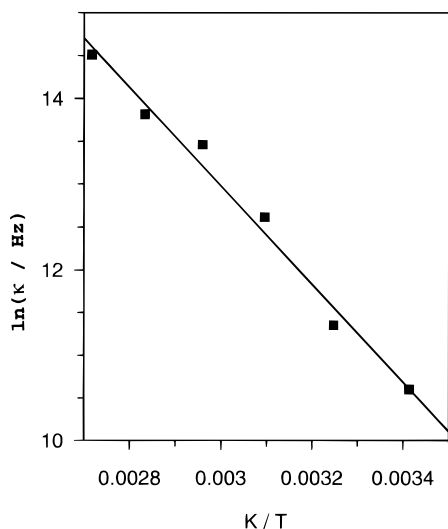


Figure 5. Graph of $\ln(\kappa/s^{-1})$ versus T^{-1}/K^{-1} for the cyclohexane ring inversion process of C_6D_{12} within the H-ZSM-5 host structure.

293 K, the line shape depends on the value of the echo delay τ , suggesting that within this temperature range a dynamic process (in addition to motions A–C) occurs in the intermediate motion regime. At 368 K, the 2H NMR spectrum at $\tau = 13 \mu s$ (an almost axially symmetric powder pattern (Figure 3)) can be accounted for by a single deuteron, without requiring us to invoke separate subspectra for axial and equatorial deuterons. This implies that the additional motion in the intermediate motion regime involves exchange of deuterons between the axial and equatorial positions (i.e., exchange between the orientations of the C–D_{ax} and C–D_{eq} bonds and hence between the z-axes of the effective V^{PAS} tensors for the axial and equatorial deuterons that result from motions A–C). Clearly, this additional motion constitutes ring inversion of the C_6D_{12} molecule. To simulate the ring inversion of the C_6D_{12} molecule, we consider (as discussed in ref 6) an exchange between two sites for which the z-axes of the V^{PAS} tensors are antiparallel but the magnitudes of V_{zz} are different, with $|V_{zz}(eq)| \approx |V_{zz}(ax)|/3$. In practice, optimal agreement between the calculated and experimental line shapes is obtained for $|\chi^*(ax)| = 51$ kHz, $\eta^*(ax) = 0$ and $|\chi^*(eq)| = 16.5$ kHz, $\eta^*(eq) = 0$. These values for $|\chi^*(ax)|$ and $|\chi^*(eq)|$ can be regarded as the effective quadrupole interaction parameters for axial and equatorial deuterons resulting from motions A–C occurring simultaneously on time scales that are rapid relative to the 2H NMR time scale.

The rate (κ) of the C_6D_{12} ring inversion process has been determined as a function of temperature by fitting independently (see Figures 3 and 4) the 2H NMR spectrum recorded at each temperature and for each of the echo delays $\tau = 13 \mu s$ and $\tau = 200 \mu s$. As shown in Figures 3 and 4, the sets of $\kappa(T)$ that provide the best fits of the experimental 2H NMR line shapes for $\tau = 13 \mu s$ and $\tau = 200 \mu s$ are in close agreement, giving further support to the validity of the proposed dynamic model. On the assumption of Arrhenius behavior (i.e., $\kappa = A \exp[-E_a/(RT)]$) for the temperature dependence of κ , the activation parameters for the C_6D_{12} ring inversion process are estimated (from a graph of $\ln(\kappa/s^{-1})$ versus T^{-1}/K^{-1} ; Figure 5) to be $E_a = (48 \pm 2)$ kJ mol $^{-1}$, $A = (1.3 \pm 0.1) \times 10^{13}$ s $^{-1}$. The enthalpy of activation is estimated (from a graph of $\ln(\kappa T^{-1}/s^{-1}K^{-1})$ versus T^{-1}/K^{-1}) to be $\Delta H^\ddagger = (45 \pm 3)$ kJ mol $^{-1}$.

5. Concluding Remarks

The variable temperature solid-state 2H NMR studies reported here have provided detailed insights into the dynamic properties

of cyclohexane guest molecules included within the microporous solid host material H-ZSM-5. Specifically, the results suggest that the reorientation of the cyclohexane molecules is determined both by the molecular structure of the guest molecules and by the structural constraints imposed by the zeolite framework (with particular regard to motion C).

It is relevant to discuss motion C in more detail, since this motion directly reflects the geometry of the zeolite host structure at the points of intersection between the zigzag tunnels and the straight tunnels. It has been shown by computer simulation¹⁹ that at sufficiently low temperature the cyclohexane guest molecules prefer to reside at the sites of intersection between the zigzag and straight tunnels rather than within the tunnels. Motion C can be interpreted readily in terms of the cyclohexane molecules residing at these intersection sites, with the molecular C_3 symmetry axis, after averaging over motions A and B, oriented preferentially along the directions of the tunnel axes. The 2H NMR analysis suggests that there is a preference for the C_3 symmetry axis to be oriented in the direction of the straight tunnel rather than in the direction of the zigzag tunnel.

It is important to emphasize, however, that 2H NMR line shape analysis is sensitive only to those components of the motion that involve reorientation of the V^{PAS} tensor, and this technique cannot provide information on translational components of the motion. Thus, analysis of the 2H NMR spectra reported in this paper cannot directly indicate the extent to which the cyclohexane guest molecules translate along the tunnels of the zeolite host structure. Thus, the 2H NMR spectra are equally consistent with a dynamic model in which the cyclohexane guest molecules translate into the straight tunnels and/or zigzag tunnels but when inside these tunnels undergo no reorientational motions in addition to those described above as motion A and motion B. In such a dynamic model, the molecular reorientation described by motion C may be interpreted in terms of the reorientational processes that occur when the cyclohexane molecule reaches the point of intersection between the tunnels, including the possibility that the cyclohexane molecule diffuses from one type of tunnel into the other. It is relevant to note, however, that the proposal that the guest molecules can translate along the tunnels and undergo reorientation described by motion C at the tunnel intersections is valid only if each cyclohexane guest molecule is constrained to experience only one specific intersection site within the zeolite. If, on the other hand, the guest molecule could move from one intersection site to another (by complete translation along one of the segments of the straight tunnel or the zigzag tunnel that links two intersections), the nature of the ZSM-5 structure dictates that motion C should involve six (rather than four) possible orientations of the molecular C_3 axis. In summary, it is clear that techniques other than 2H NMR spectroscopy (for example, computer simulation²⁰ and/or incoherent quasielastic neutron scattering) are required to assess the translational aspects of the motion of the cyclohexane guest molecules in this inclusion compound and thus to allow a definitive discrimination between the dynamic models speculated above.

On the basis of 2H NMR line shape analysis, the activation energy (E_a) for the ring inversion process for C_6D_{12} guest molecules inside the H-ZSM-5 host structure is estimated to be 48 ± 2 kJ mol $^{-1}$ and the enthalpy of activation (ΔH^\ddagger) is estimated to be $\Delta H^\ddagger = 45 \pm 3$ kJ mol $^{-1}$. These values are in close agreement with those obtained for cyclohexane in other environments: (i) in the gas phase, $\Delta H^\ddagger = 50.6$ kJ mol $^{-1}$;²¹ (ii) in solution, $\Delta H^\ddagger = 48.1$ kJ mol $^{-1}$;²² $\Delta H^\ddagger = 43.1$ kJ mol $^{-1}$;²³ (iii) in the C_6D_{12} /thiourea inclusion compound, $E_a = 46.4$ kJ mol $^{-1}$ and $\Delta H^\ddagger = 43.9$ kJ mol $^{-1}$;⁵ (iv) in the

$\text{Cd}(\text{mtn})\text{Ni}(\text{CN})_4 \cdot 1/2 \text{C}_6\text{D}_{12}$ [mtn = $\text{CH}_3\text{NH}(\text{CH}_2)_3\text{NH}_2$] inclusion compound, $E_a = 44.7 \text{ kJ mol}^{-1}$.⁶

Thus, although the intramolecular cyclohexane ring inversion process is not affected significantly by including the cyclohexane molecule within the H-ZSM-5 host structure, the motion of the whole molecule (particularly motion C) is affected significantly by the host structure. This is evident from the significant differences in the dynamic properties reported here for cyclohexane within the H-ZSM-5 host structure in comparison with the dynamic properties of cyclohexane within the other host structures discussed in (iii) and (iv) above.

In conclusion, it is clear that the structural character of the zeolite host structure exerts significant constraints on the dynamic properties of the cyclohexane guest molecules investigated here. Extensions of the present work to investigate the dynamics of other guest molecules in microporous inorganic host structures using ^2H NMR spectroscopy are likely to reveal equally interesting insights into the constraints imposed on the motion of the guest molecules, with particular interest in guest molecules that have direct relevance with regard to catalytic applications of zeolites.

Acknowledgment. We thank Dr. R. C. Mordi for preparing the sample of $\text{C}_6\text{D}_{12}/\text{H-ZSM-5}$ used in this work, University of London Intercollegiate Research Services for providing facilities for solid-state NMR spectroscopy, Professor R. G. Griffin for providing the FASTPOWDER program, Dr. D. Lewis and Professor C. R. A. Catlow for valuable discussions, and E.P.S.R.C. and the Nuffield Foundation for financial support.

References and Notes

(1) Hoatson, G. L.; Vold, R. L. *NMR Basic Principles and Progress*; Springer-Verlag: Berlin, 1994; Vol. 32, pp 3–67.

- (2) Ripmeester, J. A.; Ratcliffe, C. I. *Spectroscopic and Computational Studies of Supramolecular Systems*; Davies, J. E. D., Ed.; Kluwer Academic Publishers: Dordrecht, 1992; pp 1–27.
- (3) Vold, R. R. *Nuclear Magnetic Resonance Probes of Molecular Dynamics*; Tycko, R., Ed.; Kluwer Academic Publishers: Dordrecht, 1994; pp 27–106.
- (4) Harris, K. D. M.; Aliev, A. E. *Chem. Br.* **1995**, 31, 132.
- (5) Poupko, R.; Furman, E.; Müller, K.; Luz, Z. *J. Phys. Chem.* **1991**, 95, 407.
- (6) Nishikiori, S.; Ratcliffe, C. I.; Ripmeester, J. A. *J. Phys. Chem.* **1990**, 94, 8098.
- (7) Silbernagel, B. G.; Garcia, A. R.; Newsam, J. M.; Hulme, R. J. *Phys. Chem.* **1989**, 93, 6506.
- (8) Meier, W. M.; Olson, D. H. *Atlas of Zeolite Structure Types*, 3rd ed.; I Butterworth-Heinemann: London, 1992.
- (9) Kärger, J.; Ruthven, D. M. *Diffusion in Zeolites and other Microporous Solids*; Wiley: New York, 1992.
- (10) Silbernagel, B. G.; Garcia, A. R.; Newsam, J. M. *Colloids Surf. A* **1993**, 72, 71.
- (11) Portsmouth, R. L.; Duer, M. J.; Gladden, L. F. *J. Chem. Soc., Faraday Trans.* **1995**, 91, 559.
- (12) Aliev, A. E.; Harris, K. D. M.; Mordi, R. C. *J. Chem. Soc., Faraday Trans.* **1994**, 90, 1323.
- (13) Davis, J. H.; Jeffrey, K. R.; Bloom, M.; Valic, M. I.; Higgs, T. P. *Chem. Phys. Lett.* **1976**, 42, 390.
- (14) Wittebort, R. J.; Olejniczak, E. T.; Griffin, R. G. *J. Chem. Phys.* **1987**, 86, 5411.
- (15) Greenfield, M. S.; Ronemus, A. D.; Vold, R. L.; Vold, R. R.; Ellis, P. D.; Raidy, T. R. *J. Magn. Reson.* **1987**, 72, 89.
- (16) Rowell, J.; Phillips, W.; Melby, L.; Panar, M. *J. Chem. Phys.* **1965**, 41, 3442.
- (17) Barnes, R. G.; Bloom, J. W. *J. Chem. Phys.* **1972**, 57, 3082.
- (18) Ronemus, A. D.; Vold, R. R.; Vold, R. L. *J. Chem. Soc., Faraday Trans.* **1988**, 84, 3761.
- (19) Lewis, D.; Aliev, A. E.; Catlow, C. R. A.; Harris, K. D. M. Manuscript in preparation.
- (20) Lewis, D.; Aliev, A. E.; Catlow, C. R. A.; Harris, K. D. M. Research in progress.
- (21) Ross, B. D.; True, N. S. *J. Am. Chem. Soc.* **1983**, 105, 1382.
- (22) Hofner, D.; Lesko, S. A.; Binsch, G. *Org. Magn. Reson.* **1978**, 22, 179.
- (23) Poupko, R.; Luz, Z. *J. Chem. Phys.* **1981**, 75, 1675.